performed with Lipofectamine Plus reagent (Invitrogen) in accordance with the manufacturer's instructions. For cell death analysis with HEK293T and Neuro-2a cells, transfection efficiency was monitored with co-transfected 50 ng of pEGFP-C2 (Clontech), and confirmed that the efficiency was more than 75% before analysis.

Rat primary cortical neurons. Cortices were dissected from E-18 Sprague-Dawley rats' brains. Rat cortical neurons were plated into poly-D-lysine-coated 24-well plates. Mixed cultures were maintained in neurobasal medium. After 72 h of culture, 10 mM of cytosine arabinoside (Ara-C) was added to stop the proliferation of glial cells. After 72 h of Ara-C-treated, medium was replaced with fresh neurobasal medium.

Cell death assays. Cell death was assessed by Trypan blue exclusion, PI exclusion, LDH relase, Hoechst dye nuclear staining, MTT assay and caspase activity measurement.

For Trypan blue exclusion test, cells were collected and centrifuged for 10 min at 1000 r.p.m. The cell pellet was resuspended in 50 μl of DMEM, to which 50 μl of Trypan blue (0.4%) was added. Dead cells were counted by three independent hemocytometer counts.

LDH release from the cells into the medium was analyzed by the Cytotox 96 nonradioactive cytotoxicity assay (Promega). Cell viability of primary cortical neurons was determined by MTT assay (Chemicon) and LDH release into the medium. Nuclear condensation and membrane integrity loss were monitored by observing cells under a fluorescence microscope after application of 1 μg/ml Hoechst dye 33258 and 4 μg/ml PI. Caspase 3 activities of cells were measured with Caspase 3 Assay Kit (Sigma) in accordance with the manufacturer's instructions. For each experiment, data were obtained from three wells.

Statistical analyses for cell death were performed using the student's *t*-test and single-factor ANOVA, followed by Fisher's protected least-significant difference *post hoc* test. The results were confirmed in more than three independent experiments of all cell death analysis and Western blottings.

siRNA preparation. Sense and antisense strands of siRNA oligonucleotides were synthesized, and were then annealed at 95°C for 1 min. The sense sequence of siRNA-Bax is 5′-CCAAGAAGCUGAGCGAGUGdTdT-3′ and the sequence of control siRNA is 5′-GGUCUCGUAGACCGUGCACdTdT-3′.

Immunoprecipitation. For detecting the active form of Bax (Figure 5a–c), transfected HEK293T cells in 10-cm dishes were lysed in 200 μl Chaps buffer (150 mM NaCl, 10 mM HEPES at pH 7.4 and 1.0% Chaps) containing the protease inhibitors (1 : 100 dilution of protease inhibitor Cocktail; Sigma), according to the previously reported methods.[22] After pre-clearing 200 μl of the sample with 20 μl protein A-sepharose (CL-4B, 17-0780-01; Amersham Biosciences) at 4°C for 1 h, immunoprecipitation was performed by incubating 200 μl of the lysates with 2 μg of anti-Bax monoclonal antibody (clone 6A7, BD-Pharmingen) at 4°C for 2 h. Immunocomplexes in 200 μl of the lysates were precipitated with 20 μl protein A-sepharose. After extensive washing with buffer, beads were boiled in 40 μl Laemmli buffer, and 20 μl of the eluted proteins were analyzed by Western blotting. Western blotting analysis of pre-immunoprecipitation (input) and immunoprecipitated samples (IP) were performed with an anti-Bax polyclonal antibody (N-20, sc-493; Santa Cruz).

For detecting Bax-Ku70 interactions (Figure 4a and b), transfected HEK293T cells in 10-cm dishes were lysed in 200 μl Chaps buffer containing the protease inhibitors. After pre-clearing 200 μl of the sample with 20 μl protein G-sepharose (4 Fast Flow, 17-0618-01; Amersham Biosciences) at 4°C for 1 h, immunoprecipitation was performed by incubating 200 μl of the lysates with 2 μg of monoclonal anti-Bax antibody (B9, Santa Cruz) or 2 μg of monoclonal anti-Ku70 antibody (A9, Santa Cruz) at 4°C for 2 h. Immunocomplexes in 200 μl of the lysates were precipitated with 20 μL protein G-sepharose. After extensive washing with buffer, beads were boiled in 40 μl Laemmli buffer, and 20 μl of the eluted proteins were analyzed by Western blotting. Mouse IgG was used as negative control. Western blotting analysis of pre-immunoprecipitation (input) and immunoprecipitated samples (α-Bax or α-Ku70) were performed with an anti-Ku70 polyclonal antibody (H-308, sc-9033; Santa Cruz) or an anti-Bax polyclonal antibody (N-20, sc-493; Santa Cruz).

For detecting the acetylated form of Ku70 (Figures 4c and 7f), transfected HEK293T cells in 10-cm dishes were lysed in 200 μl 1% triton in phosphate-buffered saline containing the protease inhibitors and 5 μM TSA (Sigma).[12] After pre-clearing 200 μl of the sample with 20 μl protein G-sepharose at 4°C for 1 h, immunoprecipitation was performed by incubating 200 μl of the lysates with 4 μg of anti-pan-acetyl-lysine monoclonal antibody (9681S; Cell Signaling) at 4°C for 2 h. Immunocomplexes in 200 μl of the lysates were precipitated with 20 μl protein G-sepharose. After extensive washing with buffer, beads were boiled in 40 μl Laemmli buffer, and 20 μl of the eluted proteins were analyzed by Western blotting. Mouse IgG was used as negative control. Western blotting analysis of pre-immunoprecipitation (input) and immunoprecipitated samples (α-Ac-K) were performed with an anti-Ku70 polyclonal antibody (H-308, sc-9033; Santa Cruz).

For detecting the interactions of HA-polyQ (Q79C) and CBP or Ku70, Ku70 and CBP (Figure 6a–c), transfected HEK293T cells in 10-cm dishes were homogenized with 350 μl of ice-cold homogenization buffer (250 mM sucrose, 20 mM HEPES at pH 8.0, 10 mM KCl, 1.5 mM $MgCl_2$, 1 mM EDTA, 1 mM EGTA, pH 7.5 and 0.1 mM PMSF) containing the protease inhibitors. The cytosolic fraction was prepared by collecting the supernatant of the centrifuged homogenate samples at 14 000 r.p.m. for 30 min at 4°C. Immunoprecipitation was performed by incubating 300 μl of the lysates with 40 μl of anti-HA antibody-conjugated beads (HA-7, A2095; Sigma) or with 2 μg anti-Ku70 monoclonal antibody (A-9, sc-5309; Santa Cruz) at 4°C for 2 h. Immunocomplexes of anti-Ku70 monoclonal antibody in 200 μl of the lysates were precipitated with 20 μl protein G-sepharose beads (4 Fast Flow, 17-0618-01; Amersham Biosciences). After extensive washing with buffer, beads were boiled in 40 μl Laemmli buffer, and 20 μl of the eluted proteins were analyzed by Western blotting. Western blotting analysis of pre-immunoprecipitation (input) and immunoprecipitated samples (IP) were performed with an anti-HA polyclonal antibody (HA-7, H9658; Sigma), anti-CBP polyclonal antibody (C-20, sc-583; Santa Cruz) or anti-Ku70 polyclonal antibody (H-308, sc-9033; Santa Cruz).

Acknowledgements. We thank Dr. Akira Kakizuka for providing ataxin-3-expressing plasmid, Dr. Hideki Nishitoh for recombinant adenoviruses encoding Q79C and Q35C, Dr. Shinichirou Imai for providing mouse SIRT1 cDNA and Dr. Hideki Mochizuki for providing mouse tissue sample treated with MPTP as positive control of activated Bax. We also thank Ms. Keiko Kaneko, Ms. Kanae Yonetsu and Ms. Iku Sudo for their technical help. This work was supported in part by a grant from the 21st Century COE Program on Brain Integration and its Disorders to Tokyo Medical and Dental University (to YL and HM), Japan Foundation for Neuroscience and Mental Health (to YL, TY and HM), National Institute of Health (USA) (P20CA10373 to SM) and American Heart Association (to VG (predoctoral fellowship), JG (predoctoral fellowship) and SM (Grant-in-Aid)).

1. Ross CA. Polyglutamine pathogenesis: emergence of unifying mechanisms for Huntington's disease and related disorders. *Neuron* 2002; **35**: 819–822.
2. Shimohata T, Nakajima Tm, Yamada M, Uchida C, Onodera O, Naruse S. Expanded polyglutamine stretches interact with TAFII130, interfering with CREB-dependent transcription. *Nat Genet* 2000; **26**: 29–36.
3. Steffan JS, Bodai L, Pallos J, Poelman M, McCampbell A, Apostol BL *et al.* Histone deacetylase inhibitors arrest polyglutamine-dependent neurodegeneration in *Drosophila*. *Nature* 2001; **413**: 739–743.
4. Li F, Macfarlan T, Pittman RN, Chakravarti D. Ataxin-3 is a histone-binding protein with two independent transcriptional corepressor activities. *J Biol Chem* 2002; **277**: 45004–45012.
5. Deckwerth TL, Elliott JL, Knudson CM, Johnson Jr EM, Snider WD, Korsmeyer SJ. BAX is required for neuronal death after trophic factor deprivation and during development. *Neuron* 1996; **17**: 401–411.
6. Vaux DL, Korsmeyer SJ. Cell death in development. *Cell* 1999; **96**: 245–254.
7. Bae BI, Xu H, Igarashi S, Fujimuro M, Agrawal N, Taya Y *et al.* p53 mediates cellular dysfunction and behavioral abnormalities in Huntington's disease. *Neuron* 2005; **47**: 29–41.
8. Yoshida T, Tomioka I, Nagahara T, Holyst T, Sawada M, Hayes P *et al.* Bax-inhibiting peptide derived from mouse and rat Ku70. *Biochem Biophys Res Commun* 2004; **321**: 961–966.
9. Gomez JA, Gama V, Matsuyama S. Cell-permeable penta-peptides derived from Bax-inhibiting peptide. *Handbook of Cell Penetrating Peptides*, 2nd edn., CRC Press: Ulo Langel, 2006, pp 469–481.
10. Gomez J, Gama V, Yoshida T, Sun W, Hayes P, Leskov K *et al.* Bax Inhibiting Peptides (BIPs) derived from Ku70 and Cell Penetrating Penta-Peptides (CPP5s). *Biochem Soc Trans* 2007; **35**: 797–801.
11. Downs JA, Jackson SP. A means to a DNA end: the many roles of Ku. *Nat Rev Mol Cell Biol* 2004; **5**: 367–378.
12. Cohen HY, Lavu S, Bitterman KJ, Hekking B, Imahiyerobo TA, Miller C *et al.* Acetylation of the C terminus of Ku70 by CBP and PCAF controls Bax-mediated apoptosis. *Mol Cell* 2004; **13**: 627–638.
13. Cohen HY, Miller C, Bitterman KJ, Wall NR, Hekking B, Kessler B *et al.* Calorie restriction promotes mammalian cell survival by inducing the SIRT1 deacetylase. *Science* 2004; **305**: 390–392.

14. Subramanian C, Opipari Jr AW, Bian X, Castle VP, Kwok RP. Ku70 acetylation mediates neuroblastoma cell death induced by histone deacetylase inhibitors. *Proc Natl Acad Sci USA* 2005; **102**: 4842–4847.
15. Ikeda H, Yamaguchi M, Sugai S, Aze Y, Narumiya S, Kakizuka A. Expanded polyglutamine in the Machado–Joseph disease protein induces cell death in vitro and *in vivo*. *Nat Genet* 1996; **13**: 196–202.
16. Nishitoh H, Matsuzawa A, Tobiume K, Saegusa K, Takeda K, Inoue K *et al*. ASK1 is essential for endoplasmic reticulum stress-induced neuronal cell death triggered by expanded polyglutamine repeats. *Genes Dev* 2002; **16**: 1345–1355.
17. Xia H, Mao Q, Davidson BL. The HIV Tat protein transduction domain improves the biodistribution of beta-glucuronidase expressed from recombinant viral vectors. *Nat Biotechnol* 2001; **19**: 640–644.
18. Rampino N, Yamamoto H, Ionov Y, Li Y, Sawai H, Reed JC *et al*. Somatic frameshift mutations in the BAX gene in colon cancers of the microsatellite mutator phenotype. *Science* 1997; **275**: 967–969.
19. Clark HB, Burright EN, Yunis WS, Larson S, Wilcox C, Hartman B *et al*. Purkinje cell expression of a mutant allele of SCA1 in transgenic mice leads to disparate effects on motor behaviors, followed by a progressive cerebellar dysfunction and histological alterations. *J Neurosci* 1997; **17**: 7385–7395.
20. Sapp E, Schwarz C, Chase K, Bhide PG, Young AB, Penney J *et al*. Huntingtin localization in brains of normal and Huntington's disease patients. *Ann Neurol* 1997; **42**: 604–612.
21. Hirabayashi M, Inoue K, Tanaka K, Nakadate K, Ohsawa Y, Kamei Y *et al*. VCP/p97 in abnormal protein aggregates, cytoplasmic vacuoles, and cell death, phenotypes relevant to neurodegeneration. *Cell Death Differ* 2001; **8**: 977–984.
22. Hsu YT, Youle RJ. Bax in murine thymus is a soluble monomeric protein that displays differential detergent-induced conformations. *J Biol Chem* 1998; **273**: 10777–10783.
23. Nechushtan A, Smith CL, Hsu YT, Youle RJ. Conformation of the Bax C-terminus regulates subcellular location and cell death. *EMBO J* 1999; **18**: 2330–2341.
24. Upton JP, Valentijn AJ, Zhang L, Gilmore AP. The N-terminal conformation of Bax regulates cell commitment to apoptosis. *Cell Death Differ* 2007; **14**: 932–942.
25. Baur JA, Sinclair DA. Therapeutic potential of resveratrol: the *in vivo* evidence. *Nat Rev Drug Discov* 2006; **5**: 493–506.
26. Xiang J, Chao DT, Korsmeyer SJ. BAX-induced cell death may not require interleukin 1 beta-converting enzyme-like proteases. *Proc Natl Acad Sci USA* 1996; **93**: 14559–14563.
27. Zha H, Fisk HA, Yaffe MP, Mahajan N, Herman B, Reed JC. Structure-function comparisons of the proapoptotic protein Bax in yeast and mammalian cells. *Mol Cell Biol* 16; **1996**: 6494–6508.
28. Jurgensmeier JM, Krajewski S, Armstrong RC, Wilson GM, Oltersdorf T, Fritz LC *et al*. Bax- and Bak-induced cell death in the fission yeast *Schizosaccharomyces pombe*. *Mol Biol Cell* 1997; **8**: 325–339.
29. Chou AH, Yeh TH, Kuo YL, Kao YC, Jou MJ, Hsu CY *et al*. Polyglutamine-expanded ataxin-3 activates mitochondrial apoptotic pathway by upregulating Bax and downregulating Bcl-xL. *Neurobiol Dis* 2006; **21**: 333–345.
30. Wang HL, He CY, Chou AH, Yeh TH, Chen YL, Li AH. Polyglutamine-expanded ataxin-7 activates mitochondrial apoptotic pathway of cerebellar neurons by upregulating Bax and downregulating Bcl-x(L). *Cell Signal* 2006; **18**: 541–552.
31. Gama V, Yoshida T, Gomez JA, Basile DP, Mayo LD, Haas AL *et al*. Involvement of the ubiquitin pathway in decreasing Ku70 levels in response to drug-induced apoptosis. *Exp Cell Res* 2006; **312**: 488–499.
32. Imai S, Armstrong CM, Kaeberlein M, Guarente L. Transcriptional silencing and longevity protein Sir2 is an NAD-dependent histone deacetylase. *Nature* 2000; **403**: 795–800.
33. Parker JA, Arango M, Abderrahmane S, Lambert E, Tourette C, Catoire H *et al*. Resveratrol rescues mutant polyglutamine cytotoxicity in nematode and mammalian neurons. *Nat Genet* 2005; **37**: 349–350.
34. McCampbell A, Taye AA, Whitty L, Penney E, Steffan JS, Fischbeck KH. Histone deacetylase inhibitors reduce polyglutamine toxicity. *Proc Natl Acad Sci USA* 2001; **98**: 15179–15184.
35. Minamiyama M, Katsuno M, Adachi H, Waza M, Sang C, Kobayashi Y *et al*. Sodium butyrate ameliorates phenotypic expression in a transgenic mouse model of spinal and bulbar muscular atrophy. *Hum Mol Genet* 2004; **13**: 1183–1192.
36. Saitoh M, Nishitoh H, Fujii M, Takeda K, Tobiume K, Sawada Y *et al*. Mammalian thioredoxin is a direct inhibitor of apoptosis signal-regulating kinase (ASK) 1. *EMBO J* 1998; **17**: 2596–2606.

Supplementary Information accompanies the paper on Cell Death and Differentiation website (http://www.nature.com/cdd)

Research Signpost
37/661 (2), Fort P.O., Trivandrum-695 023, Kerala, India

Research Advances in Spinocerebellar Degeneration and Spastic Paraplegia, 2008: 57-68
ISBN: 978-81-308-0233-6 Editors: Yoshihisa Takiyama and Masatoyo Nishizawa

5

Chromosome 16q22.1-linked autosomal dominant cerebellar ataxia and spinocerebellar ataxia type 4, the two clinically distinct ataxias linked to the same locus

Kinya Ishikawa[1], Kevin Flanigan[2] and Hidehiro Mizusawa[3]
[1]Senior Assistant Professor and [3]Professor and Chairman, Department of Neurology and Neurological Sciences, Graduate School, Tokyo Medical and Dental University, Yushima 1-5-45, Bunkyo-ku 113-8519, Tokyo, Japan
[2]Associate Professor, Departments of Neurology and Human Genetics University of Utah, Salt Lake City, Utah, USA

Abstract

Autosomal dominant cerebellar ataxia (ADCA) is a group of neurodegenerative disorders inherited in autosomal dominant fashion. Although it is widely accepted that ADCA is heterogeneous both clinically

Correspondence/Reprint request: Dr. Kinya Ishikawa, Senior Assistant Professor, Department of Neurology and Neurological Sciences, Graduate School, Tokyo Medical and Dental University, Yushima 1-5-45, Bunkyo-ku 113-8519, Tokyo, Japan. E-mail: kishikawa.nuro@tmd.ac.jp

and genetically, varieties of clinical features seen in one given disorder could be explained by a combination of some clinical hallmarks which may clinically characterize the disorder. Here we describe spinocerebellar ataxia type 4 (SCA4) and chromosome 16q22.1-linked ADCA, the two distinct disorders linked to the same chromosomal region. Patients with spinocerebellar ataxia type 4 always show prominent sensory axonal neuropathy as well as cerebellar ataxia, while patients with 16q22.1-linked ADCA show isolated cerebellar ataxia with much later age of onset than SCA4. The two disorders also appear distinct neuropathologically: multiple system degenerations in SCA4 versus cerebellar cortical degeneration in 16q22.1-linked ADCA. A single-nucleotide change (-16C>T) in the puratrophin-1 gene, strongly associated with 16q22.1-linked ADCA, has not been seen in SCA4. Interestingly, the two disorders are limited so far in ethnically distinct populations: Scandinavians for SCA4 and Japanese for 16q22.1-linked ADCA. Are these two disorders allelic? Identification of causative gene(s) will ultimately settle this issue.

1. Introduction

Autosomal dominant cerebellar ataxia (ADCA) is a group of disorders with clinically and genetically heterogeneous conditions. As covered in this book, ADCA is divided in more than 30 disorders. Yet, the number of diseases comprising ADCA is expected to increase by identification of new responsible genes or gene loci.

In this chapter, we cover two ADCAs known to link to a small region in chromosome 16q22.1. The two disorders are, spinocerebellar ataxia type 4 (SCA4), and chromosome 16q22.1-linked ADCA. We first describe SCA4, and then 16q22.1-linked ADCA, as the order of disease identification. Finally, we describe recent progress on the pathogenesis of these disorders.

2. Spinocerebellar ataxia type 4 (SCA4)

In 1994, K. Gardner, L.J. Ptáček and their colleagues reported a five-generation family with ADCA, and showed a linkage to chromosome 16q13 (Gardner K. et al. 1994) [1]. Since this gene locus was the forth one responsible for ADCA, this family was named "spinocerebellar ataxia type 4 (SCA4)". Following their initial report, they examined a larger number of members in the same family, and refined the gene locus to a 6-cM (centi Morgan) region in the chromosome 16q22.1 [2]. These two reports are the original reports of SCA4 based on a single family.

This family resided in Utah and Wyoming in USA. They originated from Scandinavia. Clinically, the SCA4 family showed cerebellar ataxia of variable onset (19-59 years), with a mean age of onset at 39.3 years. In addition to cerebellar ataxia, the family was characterized by a distinct features compared

Table 1. A comparison of clinical features in SCA4 and 16q22.1-linked ADCA families.

	SCA4	SCA4	16q22.1-ADCA
Reference	#2	#3	
Ethnicity	American	German	Japanese
Number of patients	20	14	120
Age of onset (yrs)			
Ataxia	39.3	38.3	61.2
Hearing impairment	unknown	unknown	66.4
Frequencies of clinical signs and symptoms			
gait ataxia	95%	100%	100%
limb ataxia	95%	100%	92.6%
cerebellar speech	50.0%	100%	92.6%
nystagmus		57%	55%
muscle tonus			
normal			42.9%
reduced			57.1%
increased			0%
tendon reflex			
normal			71.4%
increased			0%
reduced			28.6%
absent	100%		0%
Babinski's sign	20%	7%	0%
tremor			14.3%
decreased vibratory sense	100%	100%	5.0%
loss of sensory nerve action potential	92.3%	100%	0%
dementia			0%
hearing impairment			42.7%

to other ADCAs. Among 20 affected individuals clinically examined, not only cerebellar ataxia, but also prominent sensory neuropathy was seen in nearly all patients [2]. Vibratory and joint-position senses were lost in all patients (100%), and pinprick sensation was also decreased in 95% of patients (Table 1). Ankle tendon reflexes were always absent, and 85% of patients also lacked reflexes in their knees. Complete areflexia was seen in 25% of patients. Sural sensory-nerve action potentials were absent in 12 out of 13 patients examined.

In addition to sensory neuropathy, dysarthria was noted in 50% of patients, and Babinski signs and distal weakness were both seen in 20% of patients. Eye movement were normal in most patients, except that slightly saccadic visual pursuit was noted in only two patients, and occasional spontaneous lateral movements with visual fixation was noted in one patient. Since previously known ADCAs commonly showed ophthalmoparesis as well as pyramidal & extrapyramidal tract signs as additional neurological features, prominent sensory disturbance with essentially normal eye movements in SCA4 appeared a very distinct combination. From a clinical standpoint, authors speculated that the main sites of degeneration should be the cerebellum and the dorsal root ganglia.

One of us (KF) and his colleagues [2] also performed fine mapping of the responsible gene by typing 5 microsatellite markers in chromosome 16q, and found that the disease in this family is tightly linked to a microsatellite marker D16S397, with a maximum two-point lod score of 5.93 at recombination (θ)=0. They also undertook detailed clinical investigation insights, and observed some family members with decreased sural nerve action potential without symptoms of sensory loss. This may indicate that subclinical neuropathy may be the earliest sign of SCA4.

The original Utah-Wyoming kindred had been the only SCA4 family known for a long time, until the second SCA4 family was identified from northern Germany in 2003 [3]. This German family also originated from Scandinavia (author's personal communication). The mean age of onset was at 38.3 $\pm$ 13.4 years, and the main clinical feature was cerebellar ataxia with prominent sensory neuropathy as in the Utah/Wyoming SCA4 family (Table 1). Of note is that, while sural nerve action potential was absent in all patients examined, reduced compound muscle action potential (CMAP) amplitude was seen in 3 out of 8 patients examined. This would indicate that motor axons are also affected in SCA4.

Since no other SCA4 families are known to date, presence of two families originated in the same area would indicate a founder effect.

Hellenbroich and others also mapped to their family around D16S397. By haplotype analysis, they observed two obligate recombinations, setting the centromeric border at D16S3019. Although telomeric recombination was not documented in their family, it was seen at D16S512 in the Utah/Wyoming

family [2]. These observations would indicate that the SCA4 gene lie in a 3.69 cM interval between D16S3019 and D16S512. This region is now considered 7.9 mega-base pair (Mb) in size by public database. Within this region, Hellenbroich Y. and his colleague found 34 different genes, and screened for mutation [4]. However, they did not find any mutation at least in the coding region of these genes.

Neuropathology has been described in one case [5]. Although only the brainstem and cerebellum was available for examination, they investigated in detail by making serial thick sections. They found that the degeneration was widespread and severe than what could be expected from ataxia and neuropathy phenotype of this disease. In the brainstem, marked neuronal loss was seen in the substantia nigra, red nucleus, ventral tegmental area, central raphe, pontine nuclei, all auditory brainstem nuclei, trochlear and abducens, principal trigeminal, spinal trigeminal, facial, superior vestibular, medial vestibular, interstitial vestibular, lateral vestibular, dorsal motor vagal, hypoglossal, and prepositus hypoglossal nuclei. Nucleus raphe interpositus, lateral reticular nuclei, reticulotegmental nucleus of the pons, the nucleus of Roller, all dorsal column nuclei, and the principal and medial subnuclei of the inferior olive were also severely affected. In the cerebellum, severe neuronal loss was seen in the Purkinje cell layer and in the fastigial nucleus. Unfortunately, spinal cord including sensory and motor nerve roots and dorsal root ganglia, and the cerebrum was not examined in this case. In addition to this, authors consider it important to wait for examinations on several other SCA4 brains to conclude the pattern of degeneration in SCA4, since clinical signs of such widespread brainstem degenerations were not reported in other patients [2]. Nevertheless, finding of widespread degeneration in this initial SCA4 autopsy case suggests that SCA4 and the chromosome 16q22.1-linked ADCA are different disease.

3. The chromosome 16q22.1-linked ADCA

The chromosome 16q22.1-linked ADCA was identified independently in Japanese. Authors (KI and HM) had collected Japanese ADCA families clinically characterized by purely cerebellar syndrome [6] (Table 1). Consistent with the clinical presentation, the magnetic resonance imaging disclosed cerebellar atrophy without obvious involvement of the brainstem (Figure 1). According to Harding's classification of ADCA, such pure cerebellar phenotype is classified as ADCA type III [7]. Screening all autosomes for 15 families with ADCA with pure cerebellar syndrome lead us to identify the first locus for the eight families to a chromosome 19p13.1-p13.2 [8]. These eight families were later diagnosed as SCA6, since they harbored trinucleotide CAG repeat expansion in the α1A voltage-dependent calcium

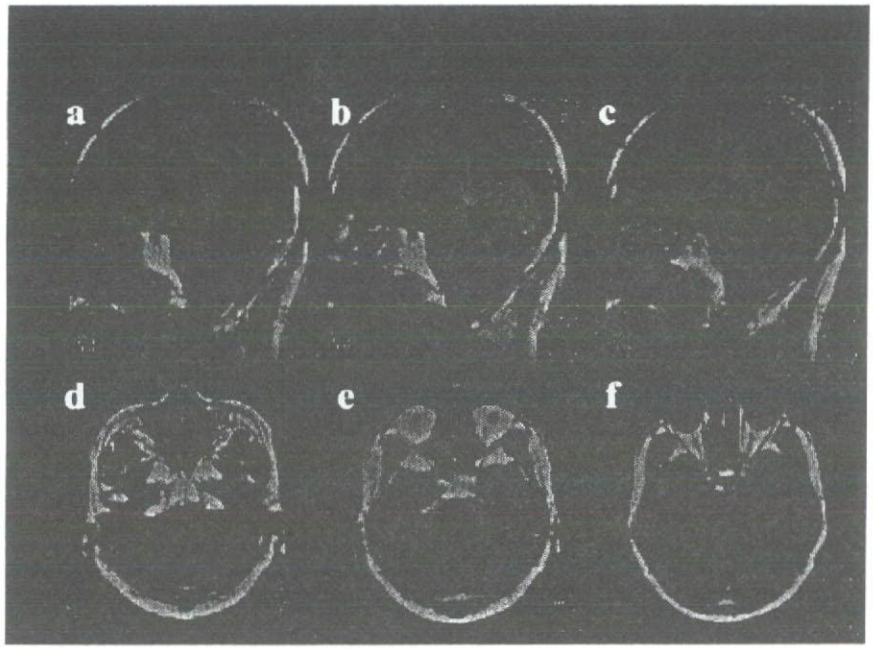

Figure 1. Magnetic resonance imaging of a patient with chromosome 16q22.1-linked ADCA. T1-weighted sagittal (a.-c.) & axial (d.-f.) brain MR images of a 58-year-old male patient 3 years after onset of ataxia. The cerebellar vermis, particularly at its upper aspect, is predominantly affected, while the brainstem is fairly well preserved.

channel gene [8-9]. We next embarked a whole genome linkage analysis for the remaining six families, and finally found that these families were linked to the *SCA4* locus in chromosome 16q13-21 [10]. This result was unexpected, since none of our families had either peripheral neuropathy or pyramidal tract signs, both of which were the clinical hallmark of SCA4. Since the clinical pictures were too distinct to consider these two diseases are allelic, we decided to coin the term "16q-linked ADCA type III" instead of a variant of SCA4.

To identify a causative gene of 16q22.1-linked ADCA, we next performed fine mapping [11], and we found a region where every patient from different families shared a same haplotype. This indicates a strong "*founder effect*" in 16q22.1-linked ADCA. Since this region with the same haplotype was demarcated by a centromeric marker, D16S3043 and a telomeric marker, D16S3095, we next constructed a physical map by independently constructing a bacterial artificial chromosome (BAC) contig [12]. By this effort, we identified several new polymorphic markers. We then applied these markers to see haplotype/allele sharing with all families, and were able to further narrow down the region with a common haplotype to a 3.8-Mb region limited by GGAA05 and D16S3095 [12].

As we collect families with ADCA type III, we encountered a large 5 generation family with 13 affected members [13]. The founder haplotype segregated with the disease in this family. Clinically, all affected individuals had

progressive cerebellar ataxia with average age of onset at 52 years. In addition, progressive hearing impairment with average age of onset at 59 years was noted in all affected individuals. During our follow-up, one of these individuals died of a natural reason at her age of 96. Detail of this patient has been described elsewhere [13-14]. To summarize, this patient noted difficulties in walking from age 70, and she gradually became ataxic. She was admitted to a nursing home at her age of 90, due to severe gait disturbance. At the age of 96, she died of natural cause. We were allowed to examine neuropathology of this patient.

Macroscopically, only the upper aspect of the vermis showed evidence of degeneration (Figure 2). Otherwise, the brain and spinal cord appeared unremarkable. Note that the degeneration appeared restricted to the upper aspect of the cerebellum, despite that the patient had the degenerative disease for 26 years. On microscopic examination, the most prominent feature was the Purkinje cell degeneration with relative preservation of molecular and granular layers. Importantly, Purkinje cells were not completely lost, but many remained with atrophic cell bodies accompanied by an amorphous structure surrounding the cell body (Figure 3). Since this amorphous material reminded us of the halo of the Lewy body, we coined the term "halo-like" amorphous structure as the peculiar Purkinje cell degeneration in 16q22.1-linked ADCA. In fact, this change was confirmed in all 16q22.1-linked ADCA patients subsequently examined neuropathologically. Since this unique feature had not been previously described, we considered that this is a neuropathological hallmark of 16q22.1-linked ADCA reflecting slow and restricted degeneration of the Purkinje cell.

Figure 2. Macroscopic view of the cerebellum of a patient with chromosome 16q22.1-linked ADCA. Consistent with MRI finding (Figure 1), degeneration is evident only at the superior vermis. Note that this individual had the disease for more than 20 years. (abopted from Ref. #15.)

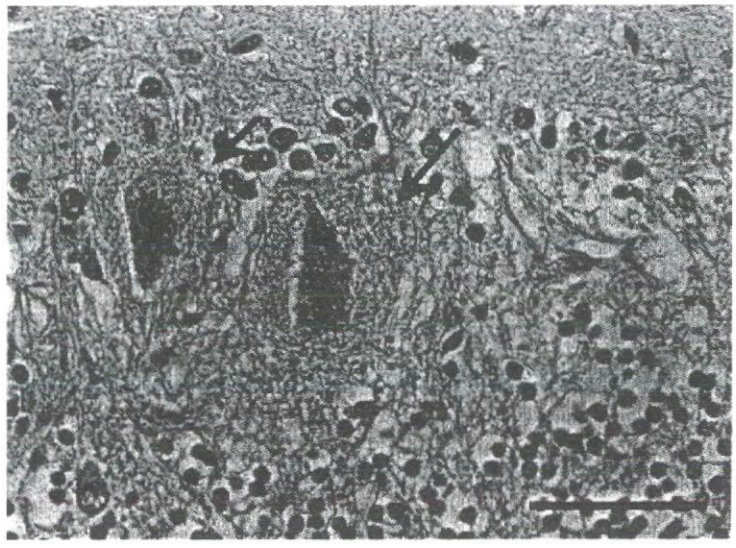

Figure 3. A peculiar Purkinje cell change in chromosome 16q22.1-linked ADCA. Note atrophic Purkinje cell bodies surrounded by so called, "halo-like" amorphous structures (arrows). (A horizontal bar measures 50 micro-meters.)

4. Identification of *puratrophin-1* genetic change in 16q22.1-linked ADCA patients

To identify the causative gene of 16q22.1-linked ADCA, we were allowed to collect 52 families from all major districts of Japan, except for Shikoku. When we further analyzed haplotypes between GGAA05 and D16S3095 [12], we prioritized the most critical interval of 16q22.1-linked ADCA to a 600 kb region between GATA01 and 17msm, because all families were found to harbor a common haplotype delimited by these two markers [15]. Twenty-two different genes were annotated in this region.

We screened all the genes annotated in this region by PCR and direct sequencing method. We also performed southern blot analysis to check for a chromosome rearrangement. From these efforts, we finally found only one genetic change which was specific for patients with 16q22.1-linked ADCA. The change was a single-nucleotide, C-to-T change seen at 16 nucleotides upstream from the putative translation initiation codon (-16C>T) of the gene, *PLEKHG4*, which we re-named as, "*puratrophin-1*"(*Purkinje cell atrophy associated protein-1*)[15](Figure 4).

Clinical features of 16q22.1-linked ADCA on 52 families were compared with those of SCA4 families (Table 1). As a definition, our families were purely cerebellar syndrome, except that approximately 40% of patients also showed hearing impairment. Notably, this symptom may be very subtle that it could only be noticed by testing with audiogram. Other groups also examined clinical features of 16q22.1-linked ADCA [16-17]. They also found that patients show

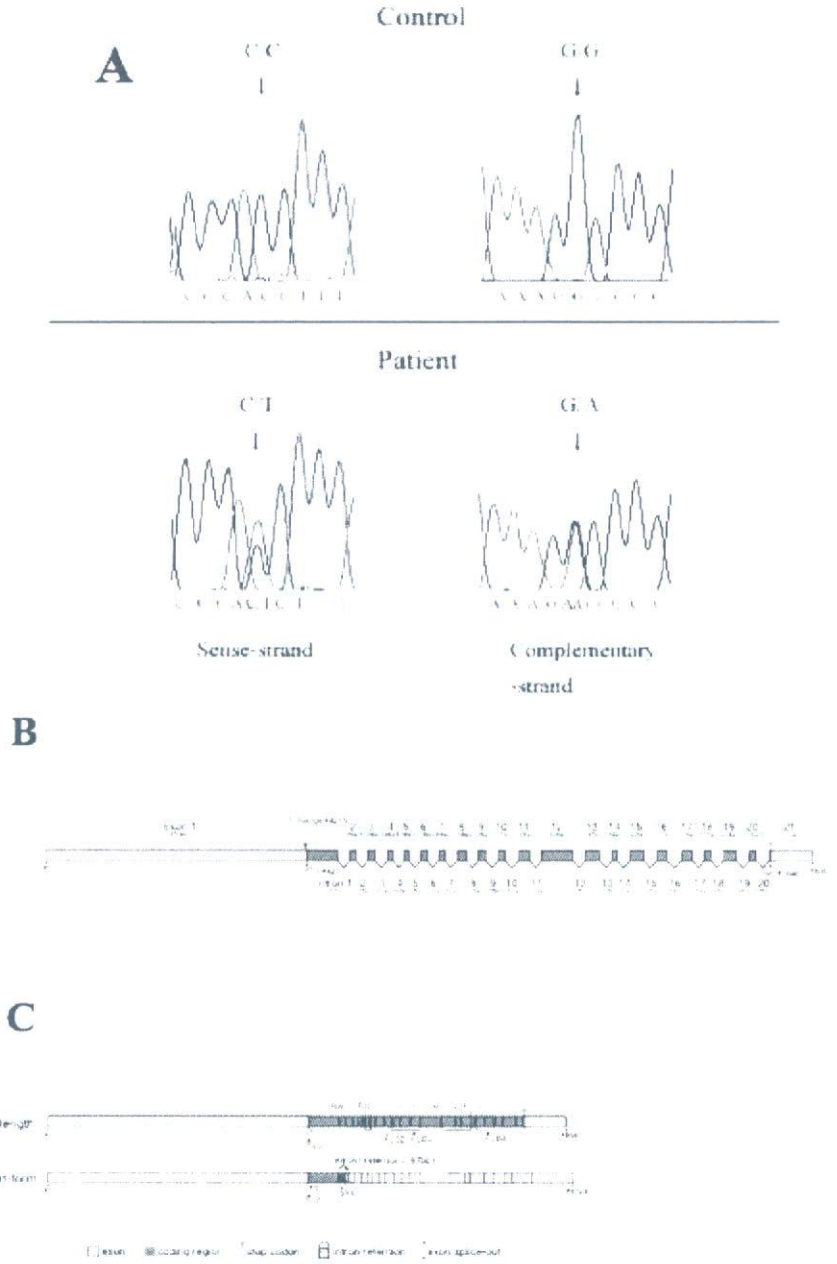

Figure 4. A -16C>T single-nucleotide change in the *puratrophin-1* gene highly associated with chromosome 16q22.1-linked ADCA. A. A single-nucleotide cytosine (C) to thymine (T) change is seen in the sense strand of patient's DNA. B. Genomic structure of the *puratrophin-1* gene. C. Full-length and short-form *puratrophin-1* mRNA. The full-length puratrphin-1 mRNA has four major domains, CRAL-TRIO, spectrin repeat, guanine nucleotide exchange factor for Rho/Rac/Cdc42-like GTPases (Rho GEF), and pleckstrin homology (PH) domains. (A-C. all adopted from Ref. #13)

"purely" cerebellar syndrome. These studies also showed that the disease frequency of 16q22.1-linked ADCA is about 10% of all ADCA in Japan. This means that 16q22.1-linked ADCA is frequent subform of ADCA, next to Machado-Joseph disease and SCA6.

5. Recent advances of pathogenesis of SCA4 and 16q22.1-linked ADCA

After an identification of a -16C>T change in the *puratrophin-1* gene as a candidate of mutation of 16q22.1-linked ADCA, one affected-individual without the -16C>T change in the *puratrophin-1* gene was found in a family in which many other affected individuals harbored the genetic change [18]. Since this "exceptional" individual harbored the same haplotype for a region centromeric to the *puratrophin-1* gene, it became possible that a true mutation may lie in a centromeric region. In addition, SCA4 subjects were not found to harbor this genetic change (*authors' unpublished data*).

Authors embarked re-screening for the common haplotype in 64 different families originated all major regions of Japan [19]. We sequenced a genome region by PCR and direct sequencing on DNA from homozygous patients harboring two disease chromosomes. We found several single-nucleotide polymorphisms (SNPs), and then examined on the rest of 64 families. When data with microsatellite markers were combined, a centromeric border was set at "SNP04", since one family showed different alleles on this SNP [19]. Consistently, microsatellite markers centromeric to SNP04 also showed alleles different from the ones common to other 16q22.1-linked ADCA families. On the other hand, other SNPs telomeric to SNP04 were conserved in all 64 families, which would indicate that the new critical region should be set at a 900 kb region between SNP04 and the -16C>T change in the *puratrophin-1* gene. Differences in alleles for microsatellite markers, such as GATA01, are now considered to be due to microsatellite instability [20]. We redefined that a true mutation must lie within the 900 kb region between SNP04 and the -16C>T change in the *puratrophin-1* gene [19]. However, another group set a critical interval of 16q22.1-linked ADCA to a 1.25-Mb region between markers 17msm and CTTT01 [21]. Since the two proposed critical interval do not overlap, further studies are needed to confirm the critical interval.

Once the mutation is identified, the issue whether or not SCA4 and 16q22.1-linked ADCA are allelic disorders will be solved. Conversely, if SCA4 and 16q22.1-linked ADCA are truly allelic diseases, efforts to check gene defects on both SCA4 and 16q22.1-linked ADCA disease chromosomes may be invaluable to pin point mutations, since any genetic changes found in a founder chromosome do not always indicate "causative".

References

1. Gardner, K., Alderson, K., Galster, B., Kaplan, C., Leppert, M., and Ptáček, L.J. 1994, Neurology, 44, Suppl 2: A361.
2. Flanigan, K., Gardner, K., Alderson, K., Galster, B., Otterud, B., Leppert, M.F., Kaplan, C., and Ptáček, L.J. 1996, Am. J. Hum. Genet., 59, 392.

3. Hellenbroich, Y., Bubel, S., Pawlack, H., Opitz, S., Vieregge, P., Schwinger, E., and Zühlke, C. 2003, J. Neurol., 250, 668.
4. Hellenbroich, Y., Pawlack, H., Rüb, U., Schwinger, E., and Zühlke, C. 2005, J. Neurol., 252, 1472.
5. Hellenbroich, Y., Gierga, K., Reusche, E., Schwinger, E., Deller, T., de Vos R.A.I., Zühlke, C., and Rüb, U. 2006, J. Neural. Transm., 113, 829.
6. Ishikawa, K., Mizusawa, H., Saito, M., Tanaka, H., Nakajima, N., Kondo, N., Kanazawa, I., Shoji, S., and Tsuji, S. 1996, Brain, 119, 1173.
7. Harding, AE. 1982, Brain, 105: 1.
8. Zhuchenko, O., Bailey, J., Bonnen, P., Ashizawa, T., Stockton, D.W., Amos, C., Dobyns, W.B., Subramony, S.H., Zoghbi, H.Y., and Lee, C.C. 1997, Nat. Genet., 15, 62.
9. Ishikawa, K., Tanaka, H., Saito, M., Ohkoshi, N., Fujita, T., Yoshizawa, K., Ikeuchi, T., Watanabe, M., Hayashi, A., Takiyama, Y., Nishizawa, M., Nakano, I., Matsubayashi, K., Miwa, M., Shoji, S., Kanazawa, I., Tsuji, S., and Mizusawa, H. 1997, Am. J. Hum. Genet., 61, 336.
10. Nagaoka, U., Takashima, M., Ishikawa, K., Yoshizawa, K., Yoshizawa, T., Ishikawa, M., Yamawaki, T., Shoji, S., and Mizusawa, H. 2000, Neurology, 54, 1971.
11. Takashima, M., Ishikawa, K., Nagaoka, U., Shoji, S., and Mizusawa H. 2001, J. Hum. Genet., 46, 167.
12. Li, M., Ishikawa, K., Toru, S., Tomimitsu, H., Takashima, M., Goto, J., Takiyama, Y., Sasaki, H., Imoto, I., Inazawa, J., Toda, T., Kanazawa, I., and Mizusawa, H. 2003, J. Hum. Genet., 48, 111.
13. Ishikawa, K., Toru, S., Tsunemi, T., Li, M., Kobayashi, K., Yokota, T., Amino, T., Owada, K., Fujigasaki, H., Sakamoto, M., Tomimitsu, H., Takashima, M., Kumagai, J., Noguchi, Y., Kawashima, Y., Ohkoshi, N., Ishida, G., Gomyoda, M., Yoshida, M., Hashizume, Y., Saito, Y., Murayama, S., Yamanouchi, H., Mizutani, T., Kondo, I., Toda, T., and Mizusawa H. 2005, Am. J. Hum. Genet., 77, 280.
14. Owada, K. Ishikawa, K., Toru, S., Ishida, G., Gomyoda, M., Tao, O., Noguchi, Y., Kitamura, K., Kondo, I., Noguchi, E., Arinami, T., and Mizusawa H. 2005, Neurology, 65, 629.
15. Ishikawa, K., and Mizusawa, H. 2006, Neuropathology, 26, 352.
16. Ouyang, Y., Sakoe, K., Shimazaki, H., Namekawa, M., Ogawa, T., Ando, Y., Kawakami, T., Kaneko, J., Hasegawa, Y., Yoshizawa, K., Amino, T., Ishikawa, K., Mizusawa, H., Nakano, I., and Takiyama, Y. 2006, J. Neurol. Sci., 247, 180.
17. Onodera, Y., Aoki, M., Mizuno, H., Warita, H., Shiga, Y., and Itoyama, Y. 2006, Neurology, 67, 1300.
18. Ohata, T., Yoshida, K., Sakai, H., Hamanoue, H., Mizuguchi, T., Shimizu, Y., Okano, T., Takada, F., Ishikawa, K., Mizusawa, H., Yoshiura, K., Fukushima, Y., Ikeda, S., and Matsumoto, N. 2006, J. Hum. Genet., 51, 461.
19. Amino, T., Ishikawa, K., Toru, S., Ishiguro, T., Sato, N., Tsunemi, T., Murata, M., Kobayashi, K., Inazawa, J., Toda, T., and Mizusawa, H. J. Hum. Genet. 2007;52(8):643-9. Epub 2007 Jul 5.

20. Ikeda, Y., Dalton, J.C., Moseley, M.L., Gardner, K.L., Bird, T.D., Ashizawa, T., Seltzer, W.K., Pandolfo, M., Milunsky, A., Potter, N.T., Shoji, M., Vincent, J.B., Day, J.W., and Ranum, L.P. 2004, Am. J. Hum. Genet., 75, 3.
21. Hirano, R., Takashima, H., Okubo, R., Tajima, K., Okamoto, Y., Ishida, S., Tsuruta, K., Arisato, T., Arata, H., Nakagawa, M., Osame, M., and Arimura, K. 2004, Neurogenetics, 5, 215.

第16番染色体長腕連鎖型脊髄小脳変性症

石川欽也　水澤英洋

Clinical Neuroscience 別冊

Vol. 25 No. 7　2007年7月1日発行

中外医学社

第16番染色体長腕連鎖型脊髄小脳変性症

石川欽也（いしかわきんや） 東京医科歯科大学 神経内科講師
水澤英洋（みずさわひでひろ） 東京医科歯科大学大学院教授 脳神経病態学

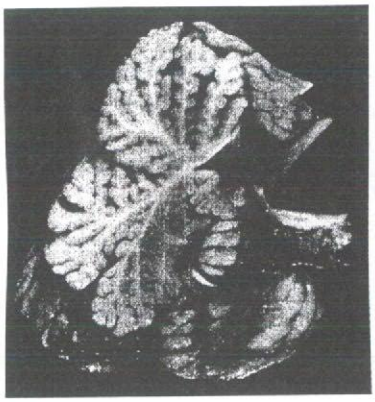

図1　16 q-ADCA 患者の小脳肉眼所見
（Owada ら[5]より）

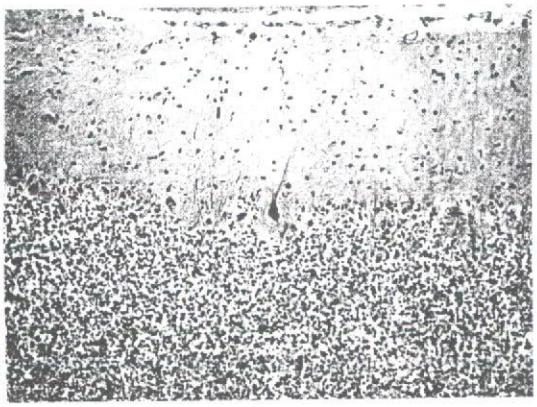

図2　16 q-ADCA 患者の小脳皮質の組織所見
小脳皮質では Purkinje 細胞の変性が他の神経細胞の脱落より目立つ．

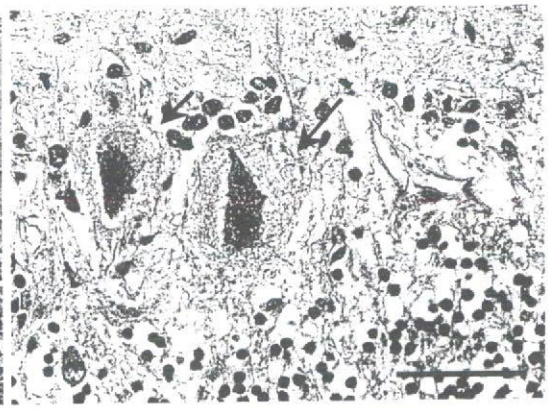

図3　16 q-ADCA 患者の小脳皮質組織所見
小脳 Purkinje 細胞は細胞体が萎縮しており，その周囲に amorphous な「帯」のような構造物（矢印）がみられる．（ヘマトキシリン・エオジン染色；スケール：50 μm）

はじめに

脊髄小脳変性症には，遺伝型と非遺伝型（孤発型）があり，前者はさらに細かく分類でき，常染色体優性遺伝型のものだけでも30に上る病型があることがわかっている[1,2]．筆者らはこれまで本邦に存在する原因不明の遺伝性脊髄小脳変性症について研究を進め，第16番染色体長腕に連鎖する病型（16 q 22.1-linked autosomal dominant cerebellar ataxia；16 q-ADCA）を見出した[3]．この病型は，既に SCA 4 という末梢神経障害を主要徴候とする米国の1家系と同じ領域に連鎖する[4]．頻度としては当初の予想を上回って本邦でかなり高く，われわれの解析結果では Machado-Joseph 病や脊髄小脳失調症6型（SCA 6）についで多く，さらに神経病理的にはこれまで記載されたことのない特徴的な所見がみられた．本稿ではこの神経病理所見について解説する．

16 q-ADCA の神経病理所見

われわれは高齢発症の純粋小脳失調症の範疇に属する家系を多数集積し経過を追跡しているうちに，ある家系の患者の病理学的検索を行える機会を得た[5]．これが SCA 4 を含めて16番染色体長腕に連鎖する2病型の中での最初の病理報告となった．患者は70歳頃に歩行障害で発症し，緩徐に小脳失調が進行し25年程度経過した96歳で老衰のために死亡した症例である．

肉眼的には小脳虫部上面が軽度萎縮していた以外は目立った変化はなかった（図1）．組織学的には，小脳皮質の変性，特に Purkinje 細胞の数が減少していることが最も目立つ所見であった（図2）．しかし25年という経過の割に変性の程度は決して強いとはいえず，小脳皮質の3層がともに変性していたのは肉眼的に萎縮のみられた小脳虫部上面にほぼ限られていた．すなわち，Purkinje 細胞の脱落に比べて，顆粒細胞や分子層の菲薄化は軽微にみえ，Purkinje 細胞がこの疾患で最も障害されやすいことがわかった．また重要なことに，残存する Purkinje 細胞ではしばしばその細胞体が萎縮し，細胞体の周囲にはエオジン好性に染まる顆粒状構造物が集まり，まるで「帯」のように細胞体を取り巻いていた（図3）．筆者らが調べた限り，このような所見はこれまでの神経病理学で記載がない新しい組織像であった．その後に判明した別の複数の16 q-ADCA 症例にもこの所見が認められ，このエオジン好性構造物は本疾患の神経病理学的特徴と考えられた．なお，その後ドイツの SCA 4 家系の病理所見が報告された[6]．それによると，SCA 4 では臨床的にも末梢神経障害や錐体路徴候がみられることに対応して，病変は小脳以外にも橋や中脳，延髄など広い範囲に及んでおり，小脳皮質には16 q-ADCA のような特徴的 Purkinje 細胞変性の像はみられない．したがって臨床上の違いのみならず，神経病理学的にも SCA 4 と16 q-ADCA は異なっていることが判明した．この違いがどのような遺伝子異常に基づいて現れるかは今後解明すべき課題である．

それではこのエオジン好性構造物の本体は何であろうか．筆者らは，小脳内では Purkinje 細胞を特異的に染めるマーカーと

0289-0585/07/¥500/論文/JCLS

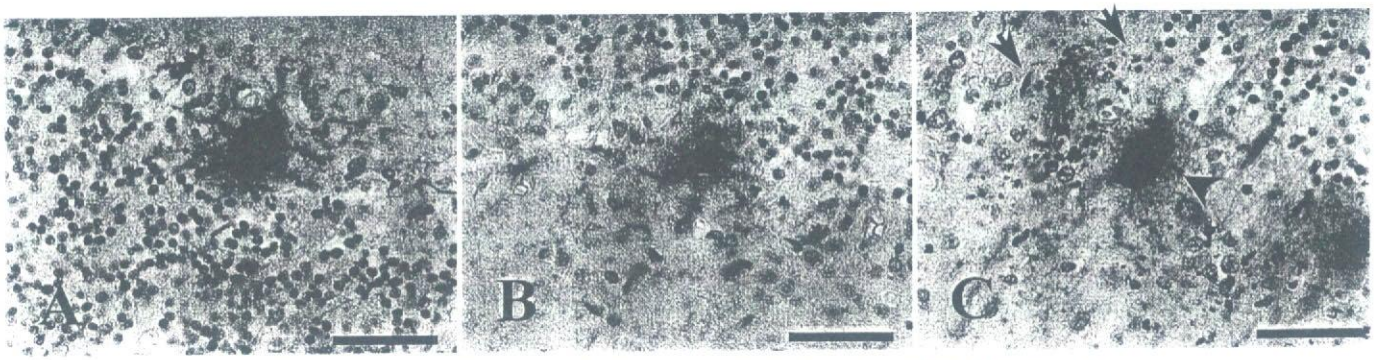

図 4　Purkinje 細胞の様々な形態変化．Calbindin D 28 k に対する免疫組織化学

A）Purkinje 細胞の“cactus-like somatic sprouting”．B）帯状構造物に担当する部分が淡く染色されている．
C）Purkinje 細胞の細胞体の周囲に濃い（矢印）あるいは淡い（矢頭）突起由来の構造物が残存している．

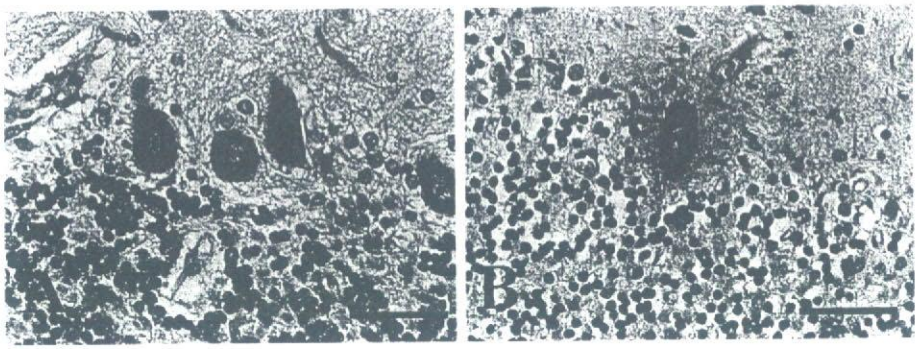

図 5　Puratrophin-1 蛋白の免疫組織化学

A）コントロール小脳皮質．
Purkinje 細胞の細胞体が均一に染色される．

B）16 q-ADCA 患者小脳皮質．
Purkinje 細胞内に強い免疫反応を示す構造がみえる．

（図 4，5 いずれも diaminobenzidine を用いた免疫組織化学；スケール：50 μm）

して有名である calbindin D 28 k[7]に対する免疫組織化学的検索を行った．その結果，Purkinje 細胞は様々な形態的変化がみられることがわかった（図 4）．まだ細胞体が萎縮していない段階でも，Purkinje 細胞の突起が細胞体から多数出現し，あたかも毬栗のようにみられる状態（“cactus-like somatic sprouting”[8]とも呼ばれている）のものから，すでに細胞体は萎縮しその細胞体から突起との連絡が不明瞭になって，あたかも突起だけが取り残されてエオジン好性構造物の中に残っているようにみえる状態まで存在しているように思われた（図 4 A～C）．特に後者の Purkinje 細胞の遺残突起がエオジン好性構造物と一致していた．

一方，このエオジン好性構造物は，シナプス前終末のマーカーである synaptophysin（Svp 38）でも免疫組織化学的に認識された．このほか，リン酸化ニューロフィラメントはエオジン好性構造物の周囲にしか存在しないことがわかった．以上のことから，Purkinje 細胞の変性とともに Purkinje 細胞の突起が細胞体周辺に出現し，おそらくこれに入力する別の神経細胞から届くシナプス前終末が集まって，このエオジン好性構造物が出現すると想像している．ちなみに，われわれが同定した puratrophin-1 は，16 q-ADCA 患者で特異的に小脳 Purkinje 細胞体内で凝集している（図 5）[9]．Puratrophin-1 蛋白はそのアミノ酸配列から pleckstrin ドメインを有し，actin と結合して Golgi 装置の形態と機能を保つ細胞骨格蛋白の一つであると考えられる[10]．しかし，なぜこの疾患の変性において細胞体から突起が出芽しやすいのかは不明である．この病理所見の根底に潜む病態の解明を行うことは，われわれに神経細胞の変性の機序に関して新しい知識をもたらしてくれると期待している．

文　献

1) Manto MU. The wide spectrum of spinocerebellar ataxias (SCAs). Cerebellum. 2005；4：2-6.
2) Cagnoli C, Mariotti C, Taroni F, et al. SCA 28, a novel form of autosomal dominant cerebellar ataxia on chromosome 18p11.22-q11.2. Brain. 2006；129：235-42.
3) Nagaoka U, Takashima M, Ishikawa K, et al. A gene on SCA 4 locus causes dominantly-inherited pure cerebellar ataxia. Neurology. 2000；54：1971-5.
4) Flanigan K, Gardner K, Alderson K, et al. Autosomal dominant spinocerebellar ataxia with sensory axonal neuropathy (SCA 4)：clinical description and genetic localization to chromosome 16q22.1. Am J Hum Genet. 1996；59：392-9.
5) Owada K, Ishikawa K, Toru S, et al. A clinical, genetic and neuropathologic study in a family with 16q-linked ADCA type III. Neurology. 2005；65：629-32.
6) Hellenbroich Y, Gierga K, Reusche E, et al. Spinocerebellar ataxia type 4 (SCA 4)：initial pathoanatomical study reveals widespread cerebellar and brainstem degeneration. J Neural Transm. 2006；113：829-43. (2005 Dec；[Epub ahead of print].)
7) Celio MR. Calbindin D28k and parvalbumin in the rat central nervous system. Neuroscience. 1990；35：375-475.
8) Urich H. The plasticity of the Purkinje cell. Clin Exp Neurol. 1984；20：203-15.
9) Ishikawa K, Toru S, Tsunemi T, et al. An autosomal dominant cerebellar ataxia linked to chromosome 16q22.1 is associated with a single-nucleotide substitution in the 5′ untranslated region of the gene encoding a protein with spectrin repeat and Rho guanine-nucleotide exchange-factor domains. Am J Hum Genet. 2005；77：280-96.
10) Lemmon MA, Ferguson KM, Abrams CS. Pleckstrin homology domains and cytoskeleton. FEBS Lett. 2002；513：71-6.